Journal of Volcanology and Geothermal Research 178 (2008) 795–806

Contents lists available at ScienceDirect

Journal of Volcanology and Geothermal Research

journal homepage: www.elsevier.com/locate/jvolgeores

Possible role of fluid overpressure in the generation of earthquake swarms in active tectonic areas: The case of the Peloritani Mts. (Sicily, Italy)

S. Giammanco [a,*], M. Palano [a], A. Scaltrito [a], L. Scarfì [a], F. Sortino [b]

[a] Istituto Nazionale di Geofisica e Vulcanologia, sezione di Catania, Piazza Roma, 2, 95123 Catania, Italy
[b] Istituto Nazionale di Geofisica e Vulcanologia, sezione di Palermo, via Ugo La Malfa 153, 90146 Palermo, Italy

ARTICLE INFO

Article history:
Received 20 February 2008
Accepted 9 September 2008
Available online 20 September 2008

Keywords:
earthquake swarm
fluid emissions
fluid-induced events
Peloritani Mts

ABSTRACT

The Peloritani Mts. (NE Sicily) are characterized by frequent seismicity. Between 1994 and 2006 more than 1000 earthquakes ($1.0 \le M_L \le 3.3$) occurred, mostly as highly clustered swarms located at shallow depth near the villages of Castroreale and Rodì Milici (western part of Peloritani Mts.). The same area is also characterized by some geothermal springs and gas vents. Using a multidisciplinary approach, data were collected on the tectonic setting, seismicity pattern and geochemical characteristics of fluid emissions, with the aim of understanding the process of earthquake swarm generation beneath the investigated area.

Most of the gases emitted in the study area, in terms of focused and/or diffuse gas emissions often associated with thermal fluids, is of mantle origin, as shown by their He isotopes ratio. On approaching the surface, deep gases interact strongly with local aquifers. An estimate of both the surface efflux of mantle-derived gases measured in focused emissions and of the P–T conditions of fluids in the local crust point to a pressurised gas source that would be located at depth of 7–12 km, corresponding to the range of hypocentral depths of seismic swarms. The complex network of tectonic structures in the area would act as high-permeability pathways for the migration of sub-crustal fluids towards the surface. This scenario could be compatible with a close interplay between pressurised mantle fluids at depth, nucleation of earthquakes due to higher-than-hydrostatic pore pressure and release of mantle-derived gases at the surface. This sequence would be repeated in time, thus producing the observed cycles in the local seismic activity.

1. Introduction

An earthquake swarm is characterized by numerous small-magnitude events within short time interval, with no predominant main shock. Earthquake swarms have been observed both in volcanically and tectonically active areas. In volcanic regions, earthquake swarms seem to be a direct consequence of subsurface magma activity (Sigmundsson et al., 1997). Such a seismicity pattern was interpreted by Hill (1977) as a consequence of magma-filled dikes existing within the brittle volume of the crust surrounding or intersected by a system of conjugate fault planes activated by magma intrusion. In active tectonic areas, earthquake swarms have been related to an increase of pore pressure caused by fluid flow (e.g. Bräuer et al., 2003). Since the early works of Irwin and Barnes (1980) and Gold and Soter (1984/85), it has become clear that there is a close relationship between active tectonic areas and the release of deep-seated fluids at the surface. Due to their high crustal permeability, faults act as preferential pathways for the upward migration and eventual release of pressurized crustal or sub-crustal gases to the atmosphere. For instance, mantle fluids are associated with the San Andreas and companion faults in central and southern-central California (Kennedy et al., 1997; Becken et al., 2008). The fluids enter the brittle fault zone at or near-lithostatic pressures and may thus contribute directly to fault-weakening high-fluid pressures at seismogenic depths (Kennedy et al., 1997; Zoback, 2000; Becken et al., 2008). Likewise, geothermal emissions have been considered as the trigger of earthquake swarms in the Bohemia/Vogtland area at the border between Germany and the Czech Republic (Špičák and Horálek, 2001; Bräuer et al., 2003).

The Peloritani Mts. in northeastern Sicily (Italy), are part of the Appennine–Maghrebian Chain, which forms the highly deformed southern margin of the Eurasian plate (Ben-Avraham et al., 1995; Lentini et al., 2000). Between 1994 and 2006, more than 1000 events were recorded in this region by a local seismic network run by the Istituto Nazionale di Geofisica e Vulcanologia, sezione di Catania (INGV-CT). Recent studies (Scarfì et al., 2005; Langer et al., 2007) showed that most of these earthquakes occurred as swarms located at about 10 km depth near the villages of Castroreale and Rodì Milici (western part of the Peloritani). This area is also characterized by the presence of some geothermal anomalies located near the villages of Terme Vigliatore and Rodì Milici. Other geothermal anomalies and gas emissions are located along the Tyrrhenian coast, especially in the area of a main tectonic structure named "Aeolian–Tindari–Letojanni

* Corresponding author. Fax: +39 095 435801.
E-mail address: giammanco@ct.ingv.it (S. Giammanco).

0377-0273/$ – see front matter © 2008 Elsevier B.V. All rights reserved.
doi:10.1016/j.jvolgeores.2008.09.005

fault system" (hereinafter ATL; Fig. 1) in the westernmost part of the Peloritani Mts. (Camarda, 2004).

In order to better understand the process of earthquake swarm generation beneath the Peloritani Mts. region, we describe the specific phenomena occurring in the region in more detail, with respect to the tectonic setting, seismicity pattern and geochemical characteristics of fluid emissions.

2. Geologic and tectonic settings

The present-day geographic framework of Sicily and surrounding areas is the result of geodynamic processes related to the convergence between the African and the Eurasian plates (Barberi et al., 1973; Boccaletti and Manetti, 1978; Patacca et al., 1990). Starting in Neogene–Quaternary, convergence processes led to the formation of

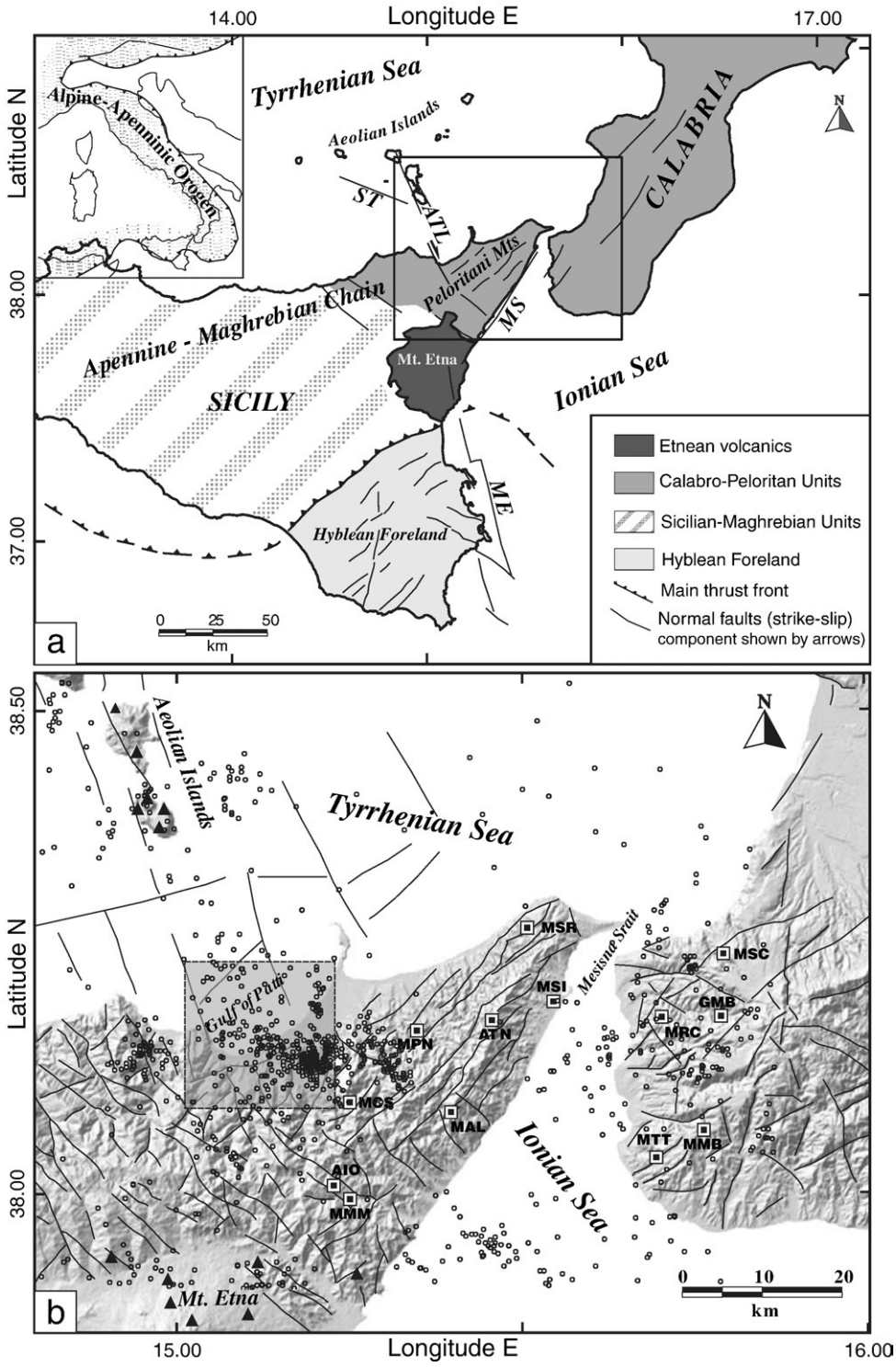

Fig. 1. a) Simplified tectonic map of Sicily and southern Calabria (from Lentini et al., 2000; Monaco and Tortorici, 2000). Abbreviations are as follows: ST, Southern Tyrrhenian fault system; ATL, Aeolian–Tindari–Letojanni fault system; MS, Messina Strait fault system; ME, Malta Escarpment fault system. The box reports the same area as in panel b. b) Structural sketch map of northeastern Sicily. Permanent seismic network is also reported: black triangles for Mt. Etna and Aeolian Islands networks and black/white boxes for NE Sicily and southern Calabria. Earthquakes spanning from 1994 to 2006 are shown with black circles. The box represents the area studied in this paper.

three distinct tectonic domains: i) the Tyrrhenian back-arc basic (extensional domain), ii) the Alpine-Apenninic orogenic belt (contractional domain) and iii) the Hyblean Foreland (Fig. 1a). Different lithosphere thicknesses and Moho depths characterize the domains. The lithosphere thickness is about 70 km beneath Sicily and about 30 km under the central Tyrrhenian Sea (Nicolich, 1989). The Moho is about 35 km deep in northeastern Sicily (Langer et al., 2007) and about 9÷12 km under the central Tyrrhenian Sea (Nicolich, 1989). Although several, often contrasting, hypotheses have been proposed to explain the current geodynamics of the area, it seems widely accepted that the causes for the extensional strain regime that has led to the formation of the Tyrrhenian oceanic basin are connected with the subduction and rollback of the Ionian plate underneath Calabria (Barberi et al., 1973; Cristofolini et al., 1985; Malinverno and Ryan, 1986; Scarascia et al., 1994; Gueguen et al., 1998; Gvirtzman and Nur, 1999; Doglioni et al., 2001; Faccenna et al., 2001, 2004; Pondrelli et al., 2004). Furthermore, the presence of a subducted slab is marked both by the occurrence of intermediate and deep earthquakes beneath the southern Tyrrhenian sea along a NW-dipping Benioff zone (Gasparini et al., 1982; Anderson and Jackson, 1987) and by a seismic high-velocity anomaly in the mantle (Selvaggi and Chiarabba, 1995).

In this context, northern Sicily, located along the convergent margin (Fig. 1a), represents the southernmost part of the Alpine-Apenninic orogenic belt. Here, the structure of the orogenic belt, called the Appennine–Maghrebian Chain, consists essentially of a nappe-pile edifice that involves distinct tectonic slices of metamorphic basement rocks (Calabro-Peloritan Arc Units), exposed in northeastern Sicily, and Mesozoic–Cenozoic sedimentary sequences (Sicilian–Maghrebian Units), exposed in central and western Sicily (Ogniben, 1960; Lentini, 1982; Catalano et al., 1996; Ortolano et al., 2005).

The Peloritani Mts. are part of the Calabro-Peloritan Arc (Fig. 1a,b). Active tectonics in this area are dominated by three main fault systems. In the eastern sector, the outcropping faults are steeply inclined surfaces (dip≥70°) dipping both eastward and westward along each side of the Messina Strait and showing prevailing dip–slip movements (Fig. 1b). This fault system, named the Messina Strait fault system, has also developed in the offshore and was probably responsible for the devastating 1908 earthquake (maximum MCS intensity of XI and approximate magnitude of 7.3), which caused a large tsunami and more than 100,000 casualties in total (Valensise and Pantosti, 1992). In the western sector, the NNW–SSE-striking faults form the onshore part of the ATL fault system. They are characterized by steeply inclined scarps (dip≥60°) that dip mostly eastward and have predominantly extensional dip–slip kinematics and subordinately left-lateral strike–slip ones (Figs. 1b and 2). Here, second-order N–S and NE–SW-striking faults splay out from the main NNW–SSE striking fault system. These faults dip both eastward and westward and show extensional dip–slip and right-lateral strike–slip kinematics (Fig. 2). The NNW–SSE faults represent the main shear zone, while the N–S and NE–SW striking faults represent tensional structures associated with the shear zone. In the northern part of the central sector both E–W- and ENE–WSW-striking fault systems occur (Fig. 2). These faults, respectively N- and NNW-dipping, are characterized by dip–slip kinematics (Di Stefano and Lentini, 1995). This tectonic configuration forms a triangular depression in the central sector of the studied area (Billi et al., 2006). The vertices of this depression are near the towns of Tindari, Barcellona P.d.G. and Novara di Sicilia (Fig. 2). In the central-southern part of this tectonic depression, the metamorphic basement (Aspromonte and Mandanici Units), outcrops extensively. The metamorphic basement is covered by turbiditic sandstones of Late Oligocene–Early Burdigalian, known as the Stilo-Capo d'Orlando Formation (Bonardi et al., 1980; Cavazza et al., 1997; Lentini et al., 2000) (Fig. 2). This formation is topped by a clay-rich mélange (Varicolori Clays) attributed either to back-thrusting (Ogniben, 1960) or to re-sedimentation (Cavazza et al., 1997). The tectono-stratigraphic sequence ends with Plio–Pleistocenic deposits formed by clay, marls, sandy clays, sand and conglomerates (Fig. 2) (Lentini et al., 2000).

3. Seismicity

We analyzed the seismicity of northeastern Sicily recorded by local networks managed by the INGV-CT (http://www.ct.ingv.it/GridTerremoti.htm). From the map shown in Fig. 1b, we observe that the seismicity is concentrated in the western part of the Peloritani Mts., between Mt. Etna and the Gulf of Patti, whereas it is almost absent along the mountain chain, up to the Messina Strait. Many of these earthquakes occurred as swarms and often as multiplets. As stated above, earthquake swarms are generally defined as clusters of earthquakes that occur in a short time span, are grouped in space and do not have a defined mainshock. In particular, multiplet events are groups of earthquakes with very similar waveforms that are coherent over several seconds (Geller and Mueller, 1980; Tsujiura, 1983a,b). These earthquakes have been commonly interpreted as repeated slips on the same fault plane (Geller and Mueller, 1980; Tsujiura, 1983a,b; Poupinet et al., 1984; Schaff et al., 1998; Nadeau and McEvilly 1999, 2004). Recently, Scarfì et al. (2005) used multiplet events that occurred near the village of Castroreale for the application of precise relocation methods. The authors found that, after relocation, formerly scattered clouds of hypocentres collapsed to small crustal volumes with an extent of no more than some hundreds of metres.

Between 1999 and 2006, about 350 earthquakes were located in the study area, defined by a rectangle with coordinates 38°.06÷38°.20 latitude (N) and 15°.03÷15°.26 longitude (E) (Fig. 3). The magnitude of these events ranged from 1.0 to 4.2. The cumulative seismic strain release and daily earthquake rate for the events located in the Peloritani Mts. are depicted in Fig. 4.

In order to improve the analysis of seismicity for the study of tectonic processes, we relocated the events by applying a relative relocation technique that can be used to produce more accurate locations than the standard absolute location procedures, particularly when seismogenic regions are dominated by spatial clustering of events. For this analysis, we retained only events having at least ten observations (P and S). Our final data set consisted of 194 well locatable events with an average of 15 body wave arrival time picks. These earthquakes were relocated using the double difference location method ("HypoDD") by Waldhauser and Ellsworth (2000) and the 1D velocity model of Langer et al. (2007). The new locations resulted in a 70% reduction in the absolute RMS residuals, with almost 75% of events having final RMS residuals smaller than 0.12 s. Very few events (about 3%) were discarded because of numerical instabilities. Relocation of these earthquakes (Fig. 3b) did not change their distribution significantly. However, looking at their spatial distribution in detail, it can be seen that most of the events are now more clustered if compared with their original locations. In particular, seismicity is concentrated in a crustal volume of a few kilometres and most of the epicentres are located near the villages of Castroreale and Rodì Milici. The depth of the foci is typically between 7 and 12 km.

Using the FPFIT code of Reasenberg and Oppenheimer (1985), we computed the focal mechanisms for earthquakes with at least ten P-wave first motion polarities available (typically, events with a magnitude ≥2.5). Where possible, P-wave polarities have been integrated with those collected from the records of stations belonging to the neighbouring Mt. Etna, Aeolian and Hyblean local networks as well as to the Italian National Seismic Network. Almost all of the focal solutions show a clear normal fault mechanism along NE–SW-striking elements (Fig. 5).

4. Geochemical survey

We focused on the chemical and isotopic characterisation of gases emitted through water as a free bubbling phase. In the study area such

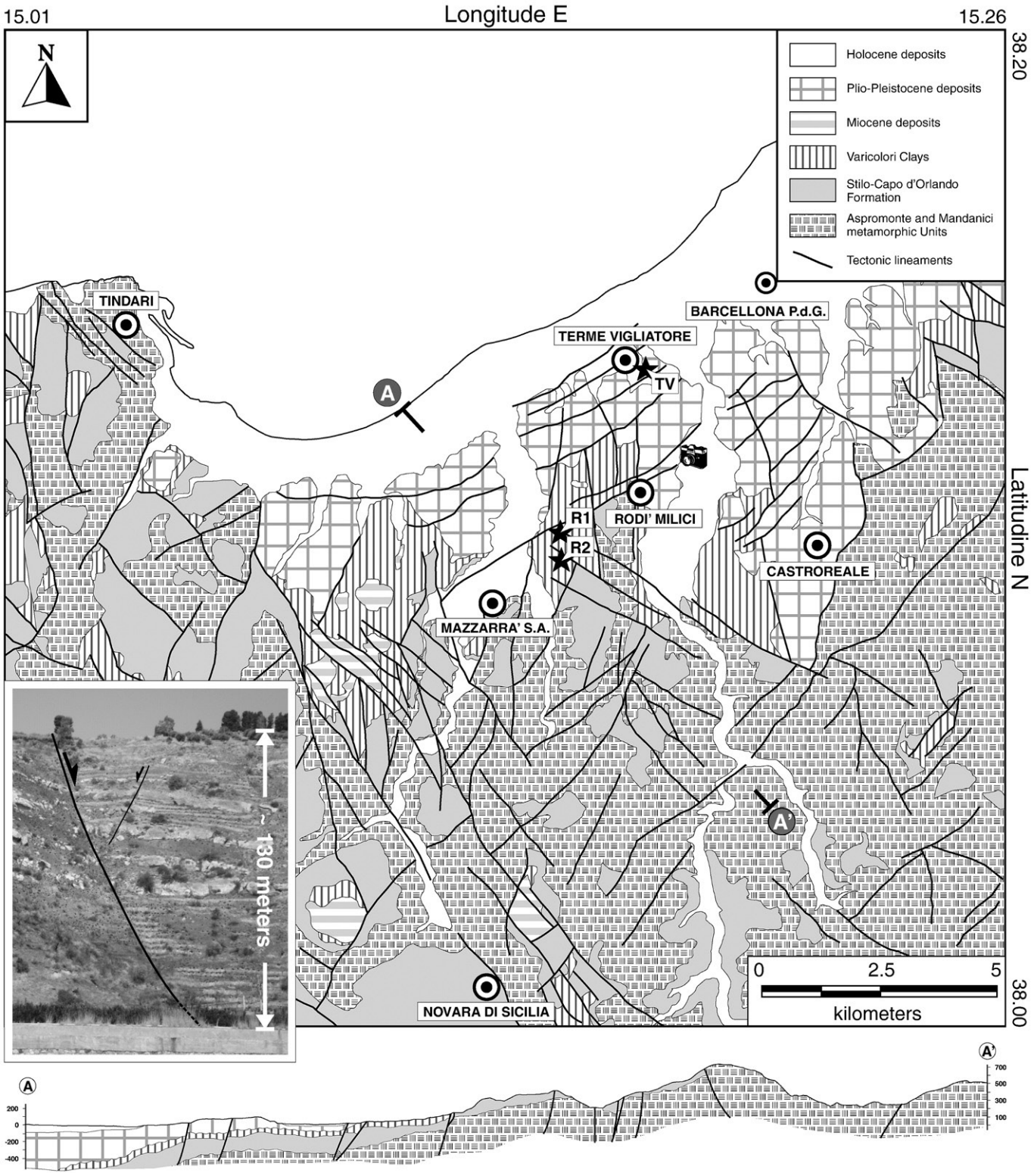

Fig. 2. Simplified structural and geological map of the investigated area. A geological section, trending NW–SE (profile A–A′) is also shown. Inset shows a photo of one of the main faults of the area together with its direction of slip. Black stars indicate the natural gas vents.

gas emissions are located both about 2–3 km SW of the village of Rodì Milici (R1 and R2 sites; Fig. 2) and near the Tyrrhenian coastline, at Terme Vigliatore (TV site; Fig. 2). In the former area, only the R1 site was sampled. In this site bubbling gases occur in five small pools of muddy water with a roughly circular shape and diameters ranging between 1 and 3 m. These pools are located on private land, and are distributed over a surface of about 22,000 m^2. At the TV site, gases bubble in water inside a well excavated for thermal water exploitation. Furthermore, gases have a much higher flux here than at the R1 and R2 sites.

Similar degassing phenomena are present in many other places in Italy and are associated with active orogenic areas (Minissale et al., 2000). In Sicily they occur both as CH_4- and CO_2-rich gas emissions accompanied by discharge of hyper-saline waters and/or mud that can

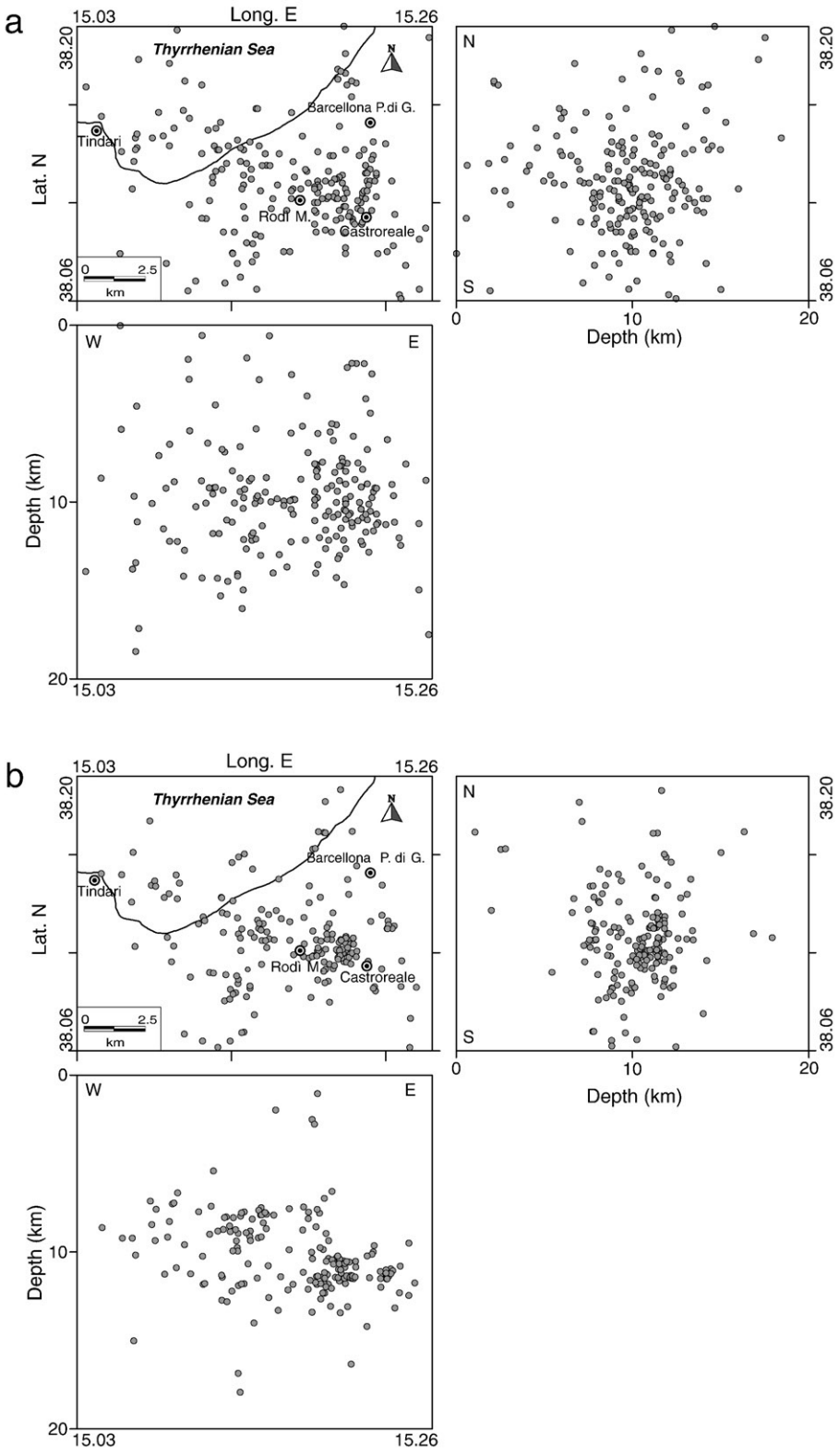

Fig. 3. Comparison between (a) the original earthquake locations of the selected data set (map view, N–S and E–W cross sections) and (b) the relocated events by use of the HypoDD code (see text for further details).

build relatively small mud cones (up to a few metres high and with a base diameter up to about ten metres) (Grassa et al., 2004; Giammanco et al., 2007). In seismogenic areas, strong increases in the flux of the gas discharged by this type of vented emissions are interpreted in terms of changes in the tectonic stress (e.g., D'Alessandro et al., 1995; Kholodov, 2002).

4.1. Methods

The gas emissions surveyed in this study include gases bubbling in water as well as diffuse emissions through soil. At the R1 site, gases were bubbling inside a small water pool (roughly circular, 3 m in diameter and about 2 m deep) (Fig. 6). The main physical–chemical

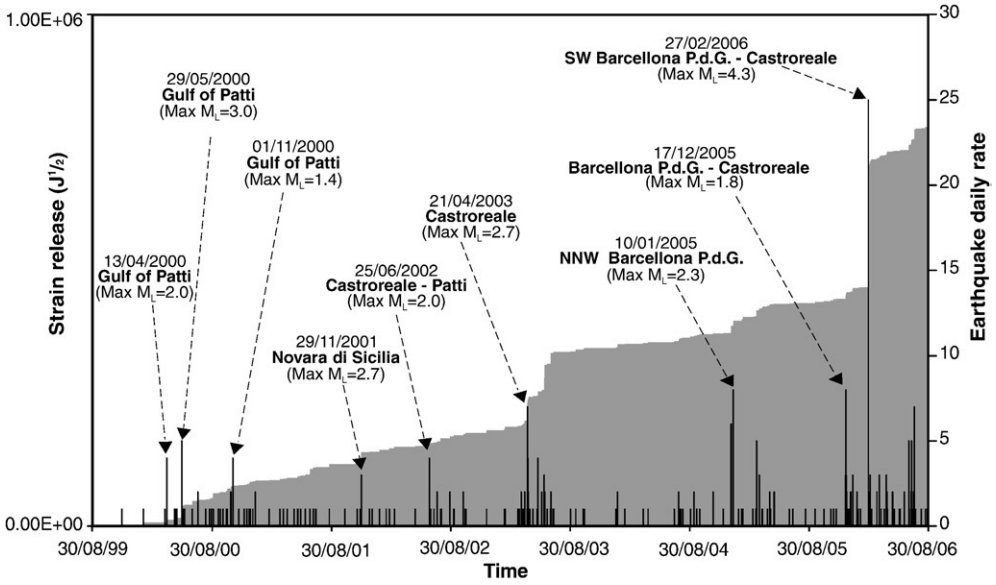

Fig. 4. Cumulative seismic strain release (grey area) and earthquake daily rate (bars) for the events located in the Peloritani Mts. area from August 1999 to August 2006. Dates of the main swarms are indicated, together with the maximum magnitude recorded.

parameters of water (temperature, pH and electrical conductivity) in this pool were measured in the field with portable electronic instruments. Values of pH and conductivity refer to the sampling temperature. Other similar water pools are present in the same site, but gas emissions inside them, when present, are weak and hardly measurable. The CO_2 efflux from the bubbling water into the main pool was estimated from the bulk mass efflux measured using an inverted funnel filled with water placed over the emission point and measuring the time required for the gas to fill it by replacing the water. The error associated with these measurements was about 15%. This efflux was then multiplied by the density and the average molar fraction of CO_2 (respectively, 1.84 kg/m^3 referred to 1013 HPa and 20 °C, and 0.13% vol), in order to obtain the values of CO_2 efflux, following the procedure described in Giammanco et al. (2007). Gases bubbling at the TV site were sampled at water surface inside a well, about 5 m below the ground surface. Gas samples were collected in glass samplers connected to the same inverted funnel used for gas mass calculations at site R1. Gas species contents in the gas samples from the R1 and TV sites were measured by gas-chromatography (see Table 1).

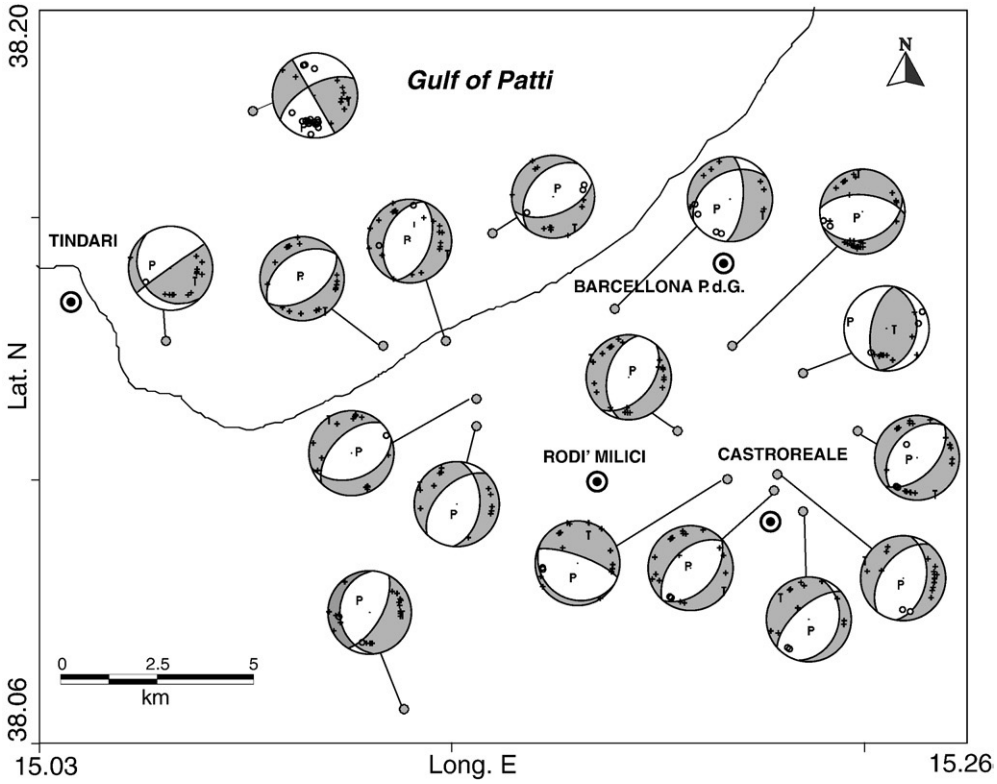

Fig. 5. Map of the investigated area with focal mechanisms of the earthquakes with magnitude >2.5.

Fig. 6. Photo showing the appearance of the water pool with the main gas vent in site R1, where gas samples were collected for their chemical and isotopic composition.

In addition, diffuse CO_2 emissions were measured at R1 site using the accumulation chamber method, which consists of measuring the rate of increase of the CO_2 concentration inside a cylindrical chamber opened at its bottom and placed on the ground surface (Tonani and Miele, 1991; Chiodini et al., 1998). The chamber has an internal fan to achieve an efficient gas mixing and is connected with a portable nondispersive infrared spectrophotometer (PP Systems, UK, mod. EGM4). The change in concentration during the initial measurement is proportional to the efflux of CO_2 (Tonani and Miele, 1991; Chiodini et al., 1998). This is an absolute method that does not require corrections linked to the physical characteristics of the soil. We tested the method in the laboratory with a series of replicate measurements of known CO_2 effluxes. The average error was about ±5%, which is assumed as a random error in the natural emission rates. The reproducibility in the range 200–1600 g m^{-2} d^{-1} was better than 5%. No such measurements were carried out at TV site because gas emission at that site is highly focused and occurs inside a large building.

In order to assess the anomaly threshold for soil CO_2 effluxes, logarithmic probability plots were used for soil CO_2 efflux (φCO_2) data, assuming a log-normal distribution of values. Sinclair (1974) argued that changes in slope in such plots are indicative of separate populations of data. For each population the arithmetic mean (M_i) and the standard deviation (σ_i) were calculated. The CO_2 output from each source recognised by means of the statistical estimations was calculated multiplying its average CO_2 efflux by the respective surface

Table 1
Chemical and isotopic composition of the gases collected in the study area. All values in ppm. Chemical analyses were carried out with a Perkin Elmer 8500 gas-chromatograph equipped with a 4 m Carbosieve S II column, using argon as carrier gas. In order to evaluate the concentration of He, H_2, O_2, N_2 and CO_2 a TCD detector was used, while CH_4 and CO concentrations were determined using an FID detector coupled with a methanizer. The limits of detection (LOD) were about 6 ppm vol. for He, 2 ppm vol. for H_2, 1 ppm vol. for CO, 2 ppm vol. for CH_4, 0.05% vol. for O_2 and 0.1% vol. for N_2. Analyses of carbon and oxygen isotopes of CO_2 were carried out by using a Finnigan Delta plus mass spectrometer. Values of carbon isotope of CO_2 are expressed in δ‰ vs. PBD, accuracy being 0.1 δ‰. Values of oxygen isotopes of CO_2 are expressed in δ‰ vs V-SMOW, accuracy being 0.2 δ‰. The $^3He/^4He$ ratios were measured by a double collector VG Masstorr FX (error±1%) and the $^4He/^{20}Ne$ ratio by a quadruple mass spectrometer VG Masstorr FX (accuracy±5%). Helium isotopic values are expressed as R/Ra, which is the $^3He/^4He$ ratio of the sample normalized to the same ratio in atmosphere ($^3He/^4He \sim 1.4\times10^{-6}$). R/Ra is the same ratio corrected for the air contamination (that in this case is negligible), following the same computation as in Sano et al. (1989)

Site	He	H_2	O_2	N_2	CO	CH_4	CO_2	R/Ra	$^4He/^{20}Ne$	R/Ra c
R1	810	<LOD	13,600	961,900	0.4	1300	1300	2.14	99.52	2.14
TV	<LOD	<LOD	<LOD	4000	<LOD	60	999,000	–	–	–

Table 2
Estimated parameters of partitioned populations of soil CO_2 effluxes measured at site R1. Subscript *i* refers to the *i*th partitioned population

Population	Number of points	$M_i \pm \sigma_i$	φCO_2 (g m^{-2} d^{-1})	S_i (m^2)	CO_2 output (kg s^{-1})
Background	13	1.04±0.24	12.4	13,970	0.002
High efflux	13	1.54±0.16	36.8	7732	0.0033
Total	26			21,702	0.0053

(S_i) obtained from a contour map computed using a Kriging spherical model, and the results are shown in Table 2.

4.2. Geochemical characterization of the gases

The gas emitted at the R1 site shows a peculiar chemical composition (Table 1). Air contamination (indicated by O_2) is low (about 1.4%), but N_2 is predominant; the CO_2 concentration is very low (1300 ppm vol) and the He content (810 ppm vol) is very high compared with that of air (5.4 ppm vol). As a consequence, the He/CO_2 ratio is 0.3, which is quite unusual for this type of gas emission and indicates that processes of chemical fractionation have strongly affected the rising gas (Caracausi et al., 2003). The physical–chemical characteristics of water in the main pool sampled at site R1 for bubbling gases indicate that water is at ambient temperature (15.3 °C), water pH is rather basic (8.57), and its electrical conductivity is 2.66 mS/cm, typical of saline water that often accompanies such gas emissions. The gas sample from site TV is significantly different from the R1 sample, in that CO_2 is the dominant gas species (99.9% vol) and He concentration is very low, typical of a hydrothermal source (Giggenbach, 1996). He isotopes were measured only at the R1 site, because the He concentration at the TV site was so low that it did not allow for a reliable analysis. The *R*/Ra value from R1 (*R*/Ra=2.14) is significantly higher than air (*R*/Ra=1) and thus points to a contribution of mantle-derived helium in the sampled gas (about 20%, assuming a pristine value of 6.1–6.7 *R*/Ra for the sub-European mantle, Dunai and Baur, 1995). Also, this value is similar to that (*R*/Ra=2.5) measured by Sano et al. (1989) in a gas sample collected at Capo Calavà, located about 20 km NW of the investigated area, where other focused gas emissions occur.

4.3. Gas output

The mass flux measurement carried out in the R1 water pool gave a value of 9.2 10^{-6} m^3 s^{-1}. The flux of CO_2 thus calculated in the gaseous phase emitted from the studied site is 2.2 10^{-6}±1.65 10^{-7} kg/s.

Furthermore, 26 soil CO_2 efflux measurements were carried out around the area of the water pools with bubbling gas, covering a surface of about 21,700 m^2. Values ranged from 4.3 to 58.8 g m^{-2} d^{-1}, with arithmetic mean of about 24.6 g m^{-2} d^{-1}. The logarithmic probability plot of the efflux data (Fig. 7) indicates one inflection point at the 49th percentile, suggesting the presence of 2 distinct populations of data. Therefore, data can be partitioned into background (<21 g m^{-2} d^{-1}) and high efflux (>21 g m^{-2} d^{-1}) end member populations (Table 2). The average soil CO_2 efflux (φCO_2) values of the two populations were 12.4 g m^{-2} d^{-1} and 36.8 g m^{-2} d^{-1}, respectively.

We used an omnidirectional spherical variogram model of the logarithmic data (with nugget=0.05, sill=1 and range=30 m) that fits the experimental values for distances shorter than the range (Fig. 8a). This model was used to produce a contour map of log φCO_2 for the 26-point survey (Fig. 8b), using Ordinary Kriging. In order to assess the quality of the gridding method, we used a cross validation technique (Goovaerts, 1997), which gave a correlation coefficient value of 0.47 for the best fit between original values and interpolated values. According to this value of the correlation coefficient, the model is not optimal in absolute terms. However, the chosen model is the best that we could produce, and the lack of a good match with the sample information in

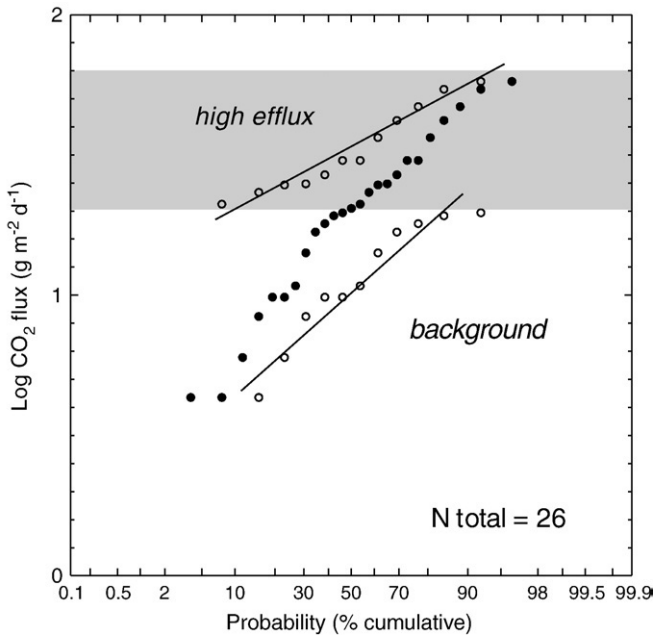

Fig. 7. Logarithmic probability plots of soil CO_2 effluxes at site R1. Original data are shown with black dots. Two statistically distinct populations are highlighted in the plot, and the respective partitioned populations are indicated with straight lines through calculated points (open circles). Parameters of each population are listed in Table 2. The grey area comprises the high degassing population that is due to deep, most likely mantle, CO_2 degassing.

this case is probably a consequence of the scarcity and/or preferential location of sampling sites, which in turn is due to logistic problems during sampling (in this case, to inaccessible private properties around the study area). Fig. 8b shows that high φCO_2 values were measured mostly in the southern part of the area, where the main pool with bubbling gas was located. Furthermore, high degassing seems to be distributed along NW–SE-oriented directions, although this could simply be the effect of local variations in shallow soil permeability, due to the very small scale of the survey. As shown in detail in Table 2, the CO_2 output from the background (i.e., biogenic) source was 2.0 10^{-3} kg s^{-1}, relevant to a surface of about 13,970 m^2, and the output from the high efflux population was about 3.3 10^{-3} kg s^{-1} (surface of about 7730 m^2).

5. Discussion

Evidence for fluid interaction and involvement with normal faults at shallow (<1–3 km) and/or deep (10 – 15 km) crustal depth has been observed in several tectonic areas (e.g. Amato et al., 1998; Sibson, 2000; Špičák and Horálek, 2001; Bräuer et al., 2003; Fitzenz and Miller, 2003). The tectonic field evidence shows that the studied area (i.e., the Tindari-Barcellona P.d.G-Novara di Sicilia tectonic depression) is mostly characterized by extensional kinematics (Fig. 2). In addition, earthquake fault plane solutions show clear normal fault mechanisms along NE–SW-striking elements (Fig. 5). This clearly demonstrates that the studied area is characterized by active extensional tectonics, at least in the 0–12 km depth range. The complex network of tectonic structures in the area could thus provide potential drainage pathways for any fluid overpressures that may develop at depth.

Migration of sub-crustal fluids towards the surface is confirmed by the widespread occurrence of over-pressured fluid emissions at the surface in the studied area as focused and/or diffuse gas emissions often associated with thermal fluids. Furthermore, isotope data on He indicate that a significant part of the fluids released at the surface derive from mantle degassing. During their ascent towards the surface, mantle fluids interact with crustal rocks and crustal fluids, particularly in the case of CO_2, and they are also contaminated with crustal ^4He. This explains why the observed R/Ra values diverge from the typical mantle range found in volcanic rocks and volcanic fluids in western Europe (Hoernle et al., 1995 and literature therein cited). Furthermore, the gas is contaminated with ^{12}C produced either by decomposition of organic material or by biogenic activity in the shallowest layers of the crust.

The large difference in chemical composition of the gases issuing from the R1 site compared with that of the gases issuing from the TV site suggests that gases from R1 are strongly depleted in the most water-soluble species (e.g., CO_2 with solubility coefficient of 759 ml/l at 25 °C and 1013 HPa, D'Amore and Truesdell, 1988) and, conversely, they are enriched in the least water-soluble gas species (e.g., CH_4 with solubility coefficient of 18 ml/l, N_2 with solubility coefficient of 12 ml/l,

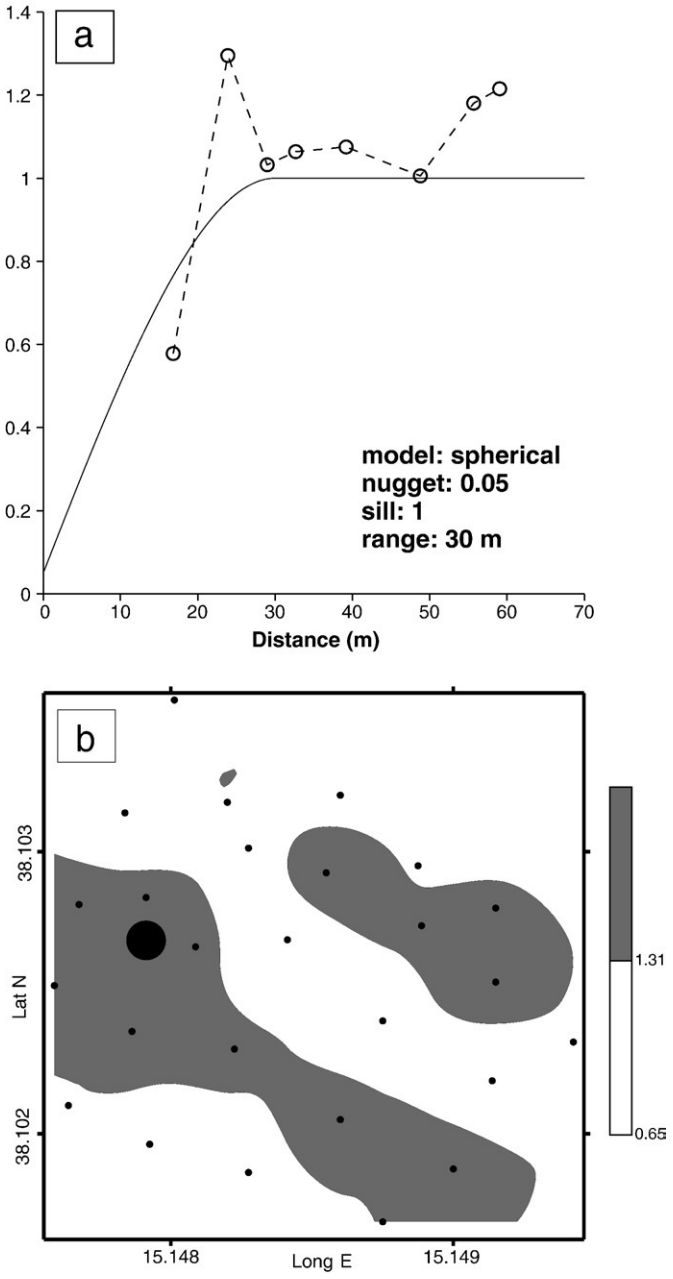

Fig. 8. a) Experimental omnidirectional semivariogram for soil efflux values measured at site R1. b) Distribution of diffuse degassing in site R1. The gray scale to the right indicates the limits (in log values of efflux expressed as g m^{-2} d^{-1}) of the two populations of CO_2 efflux values recognised with the log probability plot (Fig. 7). Small black dots indicate soil CO_2 efflux measurement points. The large black circle indicates the location of the main water pool with bubbling gas.

He with solubility coefficient of 8.75 ml/l, all at 25 °C and 1013 HPa, D'Amore and Truesdell, 1988). The opposite seems to occur in the TV gases. This is typical of environments where a widespread water table captures most of the soluble mantle-derived hot gases, in particular CO_2, and transports them downhill towards the coast where groundwaters outflow as CO_2-rich thermal springs. Confirmation of this picture comes from a recent study carried out by Grassa et al. (2006) on thermal waters from Sicily, including the TV spring water (Fig. 2). According to the results of that study, TV spring water shows a bicarbonate-alkaline composition, characterized by Na–HCO_3 chemistry and high contents of dissolved carbon and silica. The likely geochemical process governing the composition of major constituents dissolved in these waters is an intense interaction between water and silicate minerals driven by marked inflow of CO_2-rich gas in the local groundwater system. According to Grassa et al. (2006), the origin of the TV thermal waters is clearly meteoric and the amounts of dissolved CO_2 in the TV water are among the highest in the thermal springs of Sicily (about 1000 ml/l at 25 °C and 1013 HPa). Lastly, the re-calculated $\delta^{13}C$ values of the total dissolved inorganic carbon in TV waters (about −4‰ vs. V-PDB standard) are compatible with CO_2 derived from mantle degassing in the Mediterranean area ($\delta^{13}C_{CO2}$ between 0 and −2 ‰ vs. V-PDB standard, Capasso et al., 1997; Giammanco et al., 1998; Inguaggiato et al., 2000). Based on the above information, a likely geochemical model for the gases collected in the study area simulates a process of complete dissolution of CO_2 into ground water, starting from the composition of a CO_2-dominated gas with N_2, CH_4 and He contents similar to those analysed at TV. Fig. 9 shows the results of the above simulation, obtained by progressively subtracting CO_2 from the original gas and by calculating iteratively the enrichment factor (f) for the other gas species until obtaining a gas composition similar to that of the R1 site, according to the respective gas solubility in water. The gas compositions calculated at each step of the simulation were plotted as curves of concentration of CO_2, N_2, CH_4 and He in (Fig. 9). Those curves are, therefore, compatible with a process of almost complete dissolution of the original CO_2 into water accompanied by enrichment in He, N_2 and CH_4 in the residual gas passing through the water table, as justified by the large difference in the solubility constants of the gas species considered. Unfortunately, no data is available from literature regarding the exact location, dimension and depth of the aquifers in the study area.

The amount of CO_2 released through the crust in the study area is in the order of 10^{-3} kg s^{-1}, namely in the same order of magnitude as the average output of CO_2 at a global scale in tectonically active areas (Bredehoeft and Ingebritsen, 1990). This gas flux indicates gas leakage from an over-pressured source at depth, i.e., fluids within the crust attain pressures at least comparable with, if not higher than, lithostatic pressure in the depth range from the source of fluids to the surface.

The fluid pressure conditions at depth beneath the study area were estimated using some simple equations developed by Norton (1990). Assuming steady-state P–T conditions and constant volume of fluid-filled pores of crustal rocks, the variation of fluids pressure within the pores of a column of crust is assumed to be a function of the expansivity-to-compressibility ratio and of the thermal gradient:

$$\frac{dP}{dz} = \frac{\alpha_f}{\beta_f}\frac{dT}{dz} \quad (1)$$

where α_f/β_f is the isochoric coefficient of thermal pressure. According to Norton (1990), this coefficient varies between 5 and 20 bars/°C (or 0.5 to 2.0 MPa/°C) in the conditions normally found in subsiding sedimentary basins. According to Knapp and Knight (1977), for thermal gradients larger than 10 °C/km, the fluid pressure within the constant-volume pore increases to values greater than the mean confining pressure as subsidence occurs.

Data on the local thermal gradient are not readily available in literature. Information on the isothermal lines at depth beneath Peloritani Mts. can be obtained from El Ali and Giese (1978, cited in Neri et al., 1996). According to these authors, the local crust would be characterized by a thermal gradient of about 10 °C/km. Another way to obtain such data is to calculate the thermal gradient from the value of the local heat flux. The study area is located at the southern boundary of the Tyrrhenian Basin, which is characterized by anomalous heat fluxes (Zito et al., 2003). According to Zito et al. (2003), the area under study is characterized by heat fluxes of about 50 mW/m^2. This value was used to calculate the thermal gradient according to the computation made by Chapman (1986), who gives the estimate of vertical temperature profiles in the crust for many different continental tectonic provinces, down to a depth of 55 km, in the range between 40 and 90 mW/m^2. Assuming a heat flux of 50 mW/m^2, the corresponding thermal gradient would be about 15 °C/km down to a depth of 10 km, and about 11.5 °C/km at depth from 10 and 20 km. If

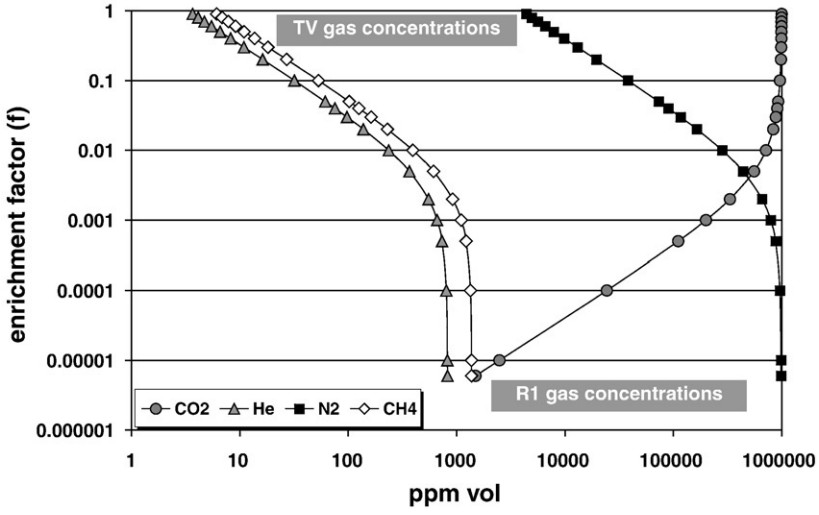

Fig. 9. Geochemical model that explains the different chemical features between the gases from R1 and those from TV sites. The model simulates a process of complete dissolution of CO_2 into water, starting from the composition of a CO_2-dominated gas with N_2, CH_4 and He contents similar to those analysed at TV. By progressively subtracting CO_2 from the original gas, the calculated concentration curves of CO_2, N_2, CH_4 and He obtained from the simulations, according to the respective gas solubility in water, indicate a process of almost total dissolution of CO_2 into water accompanied by enrichment in He, N_2 and CH_4 in the residual gas passing through the water table. At the end of the process, a gas composition similar to that of the R1 site was obtained.

we consider a depth of 10 km as the average depth of the hypocenters of the seismic swarms in the study area, then the respective crustal temperature would be between 100 and 150 °C, depending on the database considered. Based on the graphic computation made by Norton (1990), these temperatures and depth (10 km depth corresponds to lithostatic pressure of about 250 MPa, assuming a rock density of 2.9 g cm^{-3}) give a value of the isochoric coefficient of thermal pressure in the upper limit of its variability, that is between 1.8 and 2.0 MPa/°C. Therefore, the pore fluid pressure at 10 km depth would range between 180 MPa (assuming 1.8 MPa/°C and 10 °C/km) and 300 MPa (assuming 2.0 MPa/°C and 15 °C/km). These pressure values are all well above the expected value of hydrostatic pressure at the same depth (~100 MPa) and some are even above the corresponding lithostatic pressure, although the latter results are almost certainly overestimated and therefore unrealistic, at least during steady-state *T–P* conditions within the crust. These simple yet reasonable assumptions, together with the observed phenomena, point to the existence of an over-pressured source of fluids (i.e., a source of fluids at near-lithostatic pressure) beneath the study area and possibly located at depth below about 10 km. Pressurised fluids can escape from their source along high-permeability pathways in the upper crust (i.e., lithospheric faults). However, this process of mass transfer does not seem highly efficient, otherwise gas emissions would be widespread and with much lower intensity (assuming a constant mass flow from the source of fluids, a higher emissive surface reduces the unitary gas flux). As modelled for similar environments, such as the Eger rift in Germany or the Southern Iceland Seismic Zone (Bräuer et al., 2003; Zencher et al., 2006), the most likely reason for this behaviour is the presence of an impermeable transition layer or fluid trap barrier above the pressurized fluids reservoir (Fig. 10). Fluid pressure accumulation at the bottom of this layer/barrier due to partially efficient fluid release from the pressurized reservoir triggers periodic seismicity in swarms according to the models described by several authors (Bräuer et al., 2003; Fitzenz and Miller, 2003; Zencher et al., 2006; Sibson, 2007).

Such models would explain the recurrence of seismic swarms as observed in the area of this study at least during the last 8 years (Fig. 3). In our case, the above sequence of physical–chemical phenomena would affect only well-defined and restricted crustal volumes located at depth between 7 and 12 km, as shown by the foci obtained after relocation of the recorded seismic events. The above depth range is assumed as the thickness of the impermeable layer above the over-pressurized fluid reservoir (Fig. 10). In addition, the prevalence of normal faulting during swarms (Fig. 5) in the study

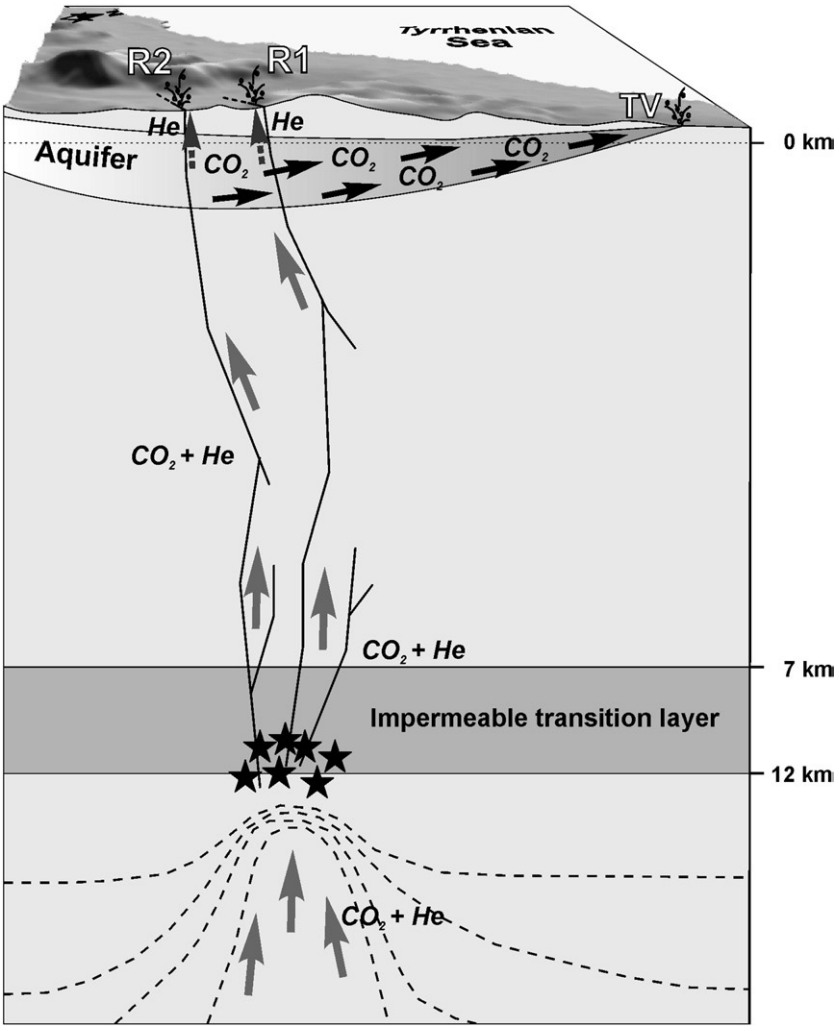

Fig. 10. Block diagram showing a simplified model of gas transport from mantle to the surface and earthquake locations in the investigated area. Mantle gas is rich in CO_2 and He and accumulates at the bottom of an impermeable transition layer, thus increasing the fluid pore pressure. Solid stars indicate the location of the seismic swarms produced by rupture of the crustal seal (impermeable transition layer) in response to fluid pressure accumulation. Arrows indicate the direction of gas flow. Dashed curves indicate theoretical pattern of isobars at depth. As the gas moves upwards along the main faults it encounters an aquifer, where CO_2 is dissolved, transported downhill with water and then released as a concentrated gas phase at site TV (Terme Vigliatore). Conversely, He can flow through the aquifer and hence reach the surface at sites R1 and R2 (Rodì Milici), being strongly enriched in the residual gas phase.

region supports the model of an impermeable transition layer (Fig. 10) pressurized from below and rupturing during earthquake swarms (Sibson, 2000).

The lack of coincidence between the epicentral area of seismic swarms and the surface outlet of sub-crustal fluids suggests that the escaping fluids do not follow vertical pathways on moving from their deep source to the surface and/or they change their starting pathways on getting closer to the surface, similar to what has been deduced for the Eger rift zone (Bräuer et al., 2003). The latter consideration has important implications on the role of the tectonic structures that allow for the migration of fluids, because it would imply the existence of at least two orders of faults (Fig. 10): i) deeper faults (depth>7 km) that drive fluid migration from their source up to, for example, the top of the impermeable transition layer; ii) shallower faults (depth<7 km) that drive fluids from the top of the transition layer to the surface.

6. Conclusions

Based on the data presented here and discussed in the previous section, we may draw the following conclusions:

(1) The study area is characterised by abnormal seismic activity, with seismic swarms of earthquakes clustered both in space and in time. The focal area is located close to Rodì Milici and focal depths are in the range between 7 and 12 km. Furthermore, the area is characterised by strong gas emissions focused in water pools and thermal springs; the origin of the gases emitted is mostly from mantle degassing;
(2) The geologic and structural framework indicates different behaviours in terms of strain release: compressive mechanisms occur far from the Tyrrhenian coast, whereas extensive mechanisms occur within the Tindari-Barcellona P.d.G-Novara di Sicilia tectonic depression, as also shown by the earthquake fault plane solutions;
(3) A geochemical model developed to explain the different chemical compositions between the gases emitted at Rodì Milici and those emitted at TV describes a system of fluids in which extreme interaction between deep gases and shallow aquifers causes dissolution of the most soluble gas species (e.g., CO_2) in water. This effect produces the CO_2-rich gas emission in the thermal waters issuing at TV. The least soluble gas species (e.g. He) are consequently enriched in the residual gas phase that flows through the water table and escapes to the surface at Rodì Milici.

The data acquired and the final multidisciplinary model describe the close interplay between pressurised mantle fluids at depth, nucleation of earthquakes due to higher-than-hydrostatic pore pressure and release of mantle-derived gases at the surface.

The temporal recurrence of seismic swarms in the study area suggests cyclic sequences of i) fluid pressure build-up; ii) near-lithostatic pore pressure propagation along isolated vertical paths; iii) drop in mechanical instability thresholds in the rocks along these paths and consequent rupture of the crustal seals; iv) fluid pressure drop after earthquakes due to rock failure and subsequent increase in crustal permeability; v) temporary recovery of hydrostatic pressure conditions within the pore fluids and increase in effective strength of the crustal rocks, likely accompanied by self-sealing of newly-formed fractures due to mineral deposition from the fracture-filling fluids after fluid pressure drop; vi) beginning of a new cycle of sealing and opening. Temporal monitoring of gas emissions, in terms of both their chemical/isotopic composition and their total output, will allow validation of the above models and hopefully will serve as a possible tool for understanding the physical/chemical phenomena that can lead to earthquake occurrence in the study area or in areas with similar characteristics.

Acknowledgements

We thank two anonymous reviewers for their constructive and helpful suggestions. We are also grateful to D. Torre, P. Trifilò and F. Trifilò owners of the private land where R1 site is located, and the staff of Parco Augusto spa at Terme Vigliatore for allowing us to carry out the gas samplings. The chemical and isotopic analyses of sampled gases were performed at the Istituto Nazionale di Geofisica e Vulcanologia, sezione di Palermo.

References

Amato, A., Azzara, R., Chiarabba, C., Cimini, G.B., Cocco, M., Di Bona, M., Margheriti, L., Mazza, S., Mele, F., Selvaggi, G., Basili, A., Boschi, E., Courboulex, F., Deschamps, A., Gaffet, S., Bittarelli, G., Chiaraluce, L., Piccinini, D., Ripepe, M., 1998. The 1997 Umbria-Marche, Italy, earthquake sequence: a first look at the main shocks and aftershocks. Geophys. Res. Lett. 25, 2861–2864.

Anderson, H., Jackson, J., 1987. The deep seismicity of the Tyrrhenian Sea. Geophys. J. R. Astron. Soc. 91, 613–637.

Barberi, F., Gasparini, P., Innocenti, F., Villari, L., 1973. Volcanism of the Southern Tyrrhenian Sea and its geodynamics implications. J. Geophys. Res. 78, 5221–5232.

Becken, M., Ritter, O., Park, S.K., Bedrosian, P.A., Weckmann, U., Weber, M., 2008. A deep crustal fluid channel into the San Andreas Fault system near Parkfield, California. Geophys. J. Int. 173, 718–732. doi:10.1111/j.1365-246X.2008.03754.x.

Ben-Avraham, Z., Lyakhovsky, V., Grasso, M., 1995. Simulation of collision zone segmentation in the central Mediterranean. Tectonophysics 243, 57–68.

Billi, A., Barberi, G., Faccenna, C., Neri, G., Pepe, F., Sulli, A., 2006. Tectonics and seismicity of the Tindari Fault System, southern Italy: crustal deformations at the transition between ongoing contractional and extensional domains located above the edge of a subducting slab. Tectonics 25, TC2006. doi:10.1029/2004TC001763.

Boccaletti, M., Manetti, P., 1978. In: Nairns, A.E.M., Knae, W.H., Stehli, F.G. (Eds.), The Tyrrhenian Sea and Adjoining Regions, in The Ocean Basins and Margins. Springer, New York, pp. 149–200.

Bonardi, G., Giunta, G., Perrone, B., Russo, M., Zuppetta, A., Ciampo, G., 1980. Osservazioni sull'evoluzione dell'Arco Calabro Peloritano nel Miocene inferiore: La Formazione di Stilo Capo d'Orlando. Boll. Soc. Geol. Ital. 99, 365–393.

Bräuer, K., Kampf, H., Sträuch, G., Weise, S.M., 2003. Isotopic evidence ($^3He/^4He$, $^{13}CCO_2$) of fluid triggered intraplate seismicity. J. Geophys. Res. 108. doi:10.1029/2002JB002077.

Bredehoeft, J.D., Ingebritsen, S.E., 1990. Degassing of carbon dioxide as a possible source of high pore pressures in the crust. In: Bredehoeft, J.D., Norton, D.L. (Eds.), The Role of Fluids in Crustal Processes. National Academy Press, Washington D.C., pp. 158–164.

Camarda, M., 2004. Soil CO_2 flux measurements in volcanic and seismic areas: Laboratory experiments and field applications. Ph.D. Thesis, University of Palermo, Italy.

Capasso, G., Favara, R., Inguaggiato, S., 1997. Chemical features and isotopic composition of gaseous manifestations on Vulcano Island (Aeolian Islands, Italy): an interpretative model of fluid circulation. Geochim. Cosmochim. Acta 61, 3425–3440.

Caracausi, A., Italiano, F., Paonita, A., Rizzo, A., Nuccio, P.M., 2003. Evidence of deep magma degassing and ascent by geochemistry of peripheral gas emissions at Mount Etna (Italy): assessment of the magmatic reservoir pressure. J. Geophys. Res. 108. doi:10.1029/2002JB002095.

Catalano, R., Di Stefano, P., Sulli, A., Vitale, F.P., 1996. Paleogeography and structure of the central Mediterranean: Sicily and its offshore area. Tectonophysics 260, 191–323.

Cavazza, W., Blenkinsop, J., Decelles, P.G., Patterson, R.T., Reinhardt, E.G., 1997. Stratigrafia e sedimentologia della sequenza sedimentaria oligocenico-quaternaria del bacino calabro-ionico. Boll. Soc. Geol. Ital. 116, 51–77.

Chapman, D.S., 1986. Thermal gradients in the continental crust. In: Dawson, J.B., Carswell, D.A., Hall, J., Wedepohl, K.H. (Eds.), The Nature of the Lower Continental Crust. Geological Society Special Publication, vol. 24, pp. 63–70.

Chiodini, G., Cioni, R., Guidi, M., Raco, B., Marini, L., 1998. Soil CO_2 flux measurements in volcanic and geothermal areas. Appl. Geochem. 13, 135–148.

Cristofolini, R., Ghisetti, F., Scarpa, R., Vezzani, L., 1985. Character of the stress field in the Calabrian Arc and Southern Apennines (Italy) as deduced by geological, seismological and volcanological information. Tectonophysics 117, 39–58.

D'Alessandro, W., De Domenico, R., Parello, F., Valenza, M., 1995. Geochemical anomalies in the gaseous phase of the mud volcanoes of Paternò–Sicily. Proc. Int. Sci. Meeting Seismic Protection, Venezia, Italy, pp. 171–175.

D'Amore, F., Truesdell, A.H., 1988. A review of solubilities and equilibrium constants for gaseous species of geothermal interest. Sci. Geol. Bull. 41, 309–332.

Di Stefano, A., Lentini, R., 1995. Ricostruzione stratigrafica e significato paleotettonico dei depositi plio-pleistocenici del margine tirrenico tra Villafranca Tirrena e Faro (Sicilia nord-orientale). Studi Geol. Camerti 1995 (2), 219–237.

Doglioni, C., Innocenti, F., Mariotti, G., 2001. Why Mt. Etna? Terra Nova 13, 25–31.

Dunai, T.J., Baur, H., 1995. Helium, neon and argon systematics of the European subcontinental mantle: implications for its geochemical evolution. Geochim. Cosmochim. Acta 59, 2767–2783.

El Ali, H., Giese, P., 1978. A geothermal profile between the Adriatic and Tyrrhenian seas: from Alps, Apennines, Hellenides. In: Closs, H., Roeder, D., Schimdt, R. (Eds.), Geodynamic Investigation along Geotraverses. Schweitzerbart, Stuttgart.

Faccenna, C., Becker, T.W., Lucente, F.P., Jolivet, L., Rossetti, F., 2001. History of subduction and back-arc extension in the central Mediterranean. Geophys. J. Int. 145, 809–820.

Faccenna, C., Piromallo, C., Crespo-Blanc, A., Jolivet, L., Rossetti, F., 2004. Lateral slab deformation and the origin of western Mediterranean arcs. Tectonics 23. doi:10.1029/2002TC001488.
Fitzenz, D.D., Miller, S.A., 2003. Fault compaction and overpressured faults: results from a 3-D model of a ductile fault zone. Geophys. J. Int. 155, 111–125.
Gasparini, P., Iannaccone, G., Scandone, P., Scarpa, R., 1982. Seismotectonics of the Calabrian Arc. Tectonophysics 84, 267–286.
Geller, R.J., Mueller, C.S., 1980. Four similar earthquakes in Central California. Geophys. Res. Lett. 7, 821–824.
Giammanco, S., Inguaggiato, S., Valenza, M., 1998. Soil and fumarole gases of Mount Etna: geochemistry and relations with volcanic activity. J. Volcanol. Geotherm. Res. 81, 297–310.
Giammanco, S., Parello, F., Gambardella, B., Schifano, R., Pezzullo, S., Galante, G., 2007. Focused and diffuse effluxes of CO_2 from mud volcanoes and mofettes south of Mt. Etna (Italy). J. Volcanol. Geotherm. Res. 165, 46–63.
Giggenbach, W.F., 1996. Chemical composition of volcanic gases. In: Scarpa, R., Tilling, R.I. (Eds.), Monitoring and Mitigation of Volcano Hazards. Springer, pp. 221–256.
Gold, T., Soter, S., 1984/85. Fluid ascent through the solid lithosphere and its relation to earthquakes. Pure Appl. Geophys. 122, 492–530.
Goovaerts, P., 1997. Geostatistics for Natural Resources Evaluation. Oxford University Press, New York. 483 pp.
Grassa, F., Capasso, G., Favara, R., Inguaggiato, S., Faber, E., Valenza, M., 2004. Molecular and isotopic composition of free hydrocarbon gases from Sicily, Italy. Geophys. Res. Lett. 31, L06607. doi:10.1029/2003GL019362.
Grassa, F., Capasso, G., Favara, R., Inguaggiato, S., 2006. Chemical and isotopic composition of waters and dissolved gases in some thermal springs of Sicily and adjacent volcanic islands, Italy. Pure Appl. Geophys. 163, 781–807. doi:10.1007/s00024-006-0043-0.
Gueguen, E., Doglioni, C., Fernandez, M., 1998. On the post-25 Ma geodynamic evolution of the western Mediterranean. Tectonophysics 298, 259–269.
Gvirtzman, Z., Nur, A., 1999. The formation of Mount Etna as the consequence of slab rollback. Nature 401, 782–785.
Hill, D.P., 1977. A model for earthquake swarms. J. Geophys. Res. 82, 1347–1352.
Hoernle, K., Zhang, Y.S., Graham, D., 1995. Seismic and geochemical evidence for large-scale mantle upwelling beneath the eastern Atlantic and western and central Europe. Nature 374, 34–39.
Inguaggiato, S., Pecoraino, G., D'Amore, F., 2000. Chemical and isotopical characterisation of fluid manifestations of Ischia Island (Italy). J. Volcanol. Geotherm. Res. 99, 151–178.
Irwin, W.P., Barnes, I., 1980. Tectonic relations of carbon dioxide discharges and earthquakes. J. Geophys. Res. 85, 3115–3121.
Kennedy, B.M., Kharaka, Y.K., Evans, W.C., Ellwood, A.D.J., DePaolo, J., Thordsen, G., Mariner, R.H., 1997. Mantle fluids in the San Andreas Fault System California. Science 278, 1278–1280.
Kholodov, V.N., 2002. Mud volcanoes: distribution regularities and genesis (Communication 2. Geological–geochemical peculiarities and formation model). Lithol. Miner. Resour., Vol. 37, No. 4, 2002, pp. 293–309. (Translated from Litologiya i Poleznye Iskopaemye, No. 4, 2002), pp. 339–358.
Knapp, R.B., Knight, J.E., 1977. Differential thermal expansion of pore fluids: Fracture propagation and microearthquake production in hot pluton environments. J. Geophys. Res. 82, 2515–2522.
Langer, H., Raffaele, R., Scaltrito, A., Scarfi, L., 2007. Estimation of an optimum Velocity Model in the Peloritani Mountains—Assessment of the variance of model parameters and variability of earthquake locations. Geophys. J. Int. 170 (3), 1151–1164. doi:10.1111/j.1365-246X.2007.03459.x.
Lentini, F., 1982. The geology of the Mt Etna basement. Mem. Soc. Geol. Ital. 23, 7–26.
Lentini, F., Catalano, S., Carbone, S., 2000. Carta geologica della Provincia di Messina. SELCA, Florence, Italy.
Malinverno, A., Ryan, W.B.F., 1986. Extension in the Tyrrhenian Sea and shortening in the Apennines as result of arc migration driven by sinking of the lithosphere. Tectonics 5, 227–254.
Minissale, A., Magro, G., Martinelli, G., Vaselli, O., Tassi, G.F., 2000. Fluid geochemical transect in the Northern Apennines (central-northern Italy): fluid genesis and migration and tectonic implications. Tectonophysics 319, 199–222.
Monaco, C., Tortorici, L., 2000. Active faulting in the Calabrian arc and eastern Sicily. J. Geodyn. 29, 407–424.
Nadeau, R.M., McEvilly, T.V., 1999. Fault slip rates at depth from recurrence intervals of repeating microearthquakes. Science 285, 718–721. doi:10.1126/science.285.5428.718.
Nadeau, R.M., McEvilly, T.V., 2004. Periodic pulsing of characteristic microearthquakes on the San Andreas Fault. Science 303, 220–222. doi:10.1126/science.1090353.
Neri, G., Caccamo, D., Cocina, O., Montalto, A., 1996. Geodynamic implications of earthquake data in the southern Tyrrhenian sea. Tectonophysics 258, 233–249.
Nicolich, R., 1989. Crustal structures from seismic studies in the frame of the European Geotraverse (southern segment) and CROP projects. In: Boriani, A., et al. (Ed.), The Lithosphere in Italy. Accad. Naz. dei Lincei, Rome, Italy, pp. 41–61.
Norton, D.L., 1990. Pore fluid pressure near magma chambers. The Role of Fluids in Crustal Processes. The National Academy of Sciences, pp. 42–49.
Ogniben, L., 1960. Nota illustrativa dello schema geologico della Sicilia nord-orientale. Riv. Min. Sicil. 64–65, 183–212.
Ortolano, G., Cirrincione, R., Pezzino, A., 2005. P–T evolution of Alpine metamorphism in the southern Aspromonte Massif (Calabria–Italy). Schweiz. Mineral. Petrogr. Mitt. 85, 31–56.
Patacca, E., Sartori, R., Scandone, P., 1990. Tyrrhenian basin and Apenninic arcs: Kinematic relations since late Tortonian times. Mem. Soc. Geol. Ital. 45, 425–451.
Pondrelli, S., Piromallo, C., Serpelloni, E., 2004. Convergence vs. Retreat in Southern Tyrrhenian Sea: insights from kinematics. Geophys. Res. Lett. 31, L0661. doi:10.1029/2003GL019223.
Poupinet, G., Ellsworth, W.L., Fréchet, J., 1984. Monitoring velocity variations in crust using earthquake doublets: an application to the Calaveras fault, California. J. Geophys. Res. 89, 5719–5731.
Reasenberg, P.A., Oppenheimer, D., 1985. FPFIT, FPPLOT and FPPAGE: Fortran computer programs for calculating and displaying earthquake fault-plane solutions. Open File Rep. U. S. Geol. Surv., Washington, pp. 85–379. 109 pp.
Sano, Y., Wakita, H., Italiano, F., Nuccio, P.M., 1989. Helium isotopes and tectonics in Southern Italy. Geophys. Res. Lett. 16, 511–514.
Scarascia, S., Lozej, A., Cassinis, R., 1994. Crustal structures of the Ligurian, Tyrrhenian and Ionian Sea and adjacent onshore areas interpreted from wide-angle seismic profile. Boll. Geofis. Teor. Appl. 36, 5–19.
Scarfì, L., Langer, H., Scaltrito, A., 2005. Relocation of microearthquake swarms in the Peloritani mountains—implications on the interpretation of seismotectonic patterns in NE Sicily, Italy. Geophys. J. Int. 163, 225–237. doi:10.1111/j.1365-246X.2005.02720.x.
Schaff, D., Beroza, G.C., Shaw, B.E., 1998. Postseismic response of repeating aftershocks. Geophys. Res. Lett., 25, 4549–4552.
Selvaggi, G., Chiarabba, C., 1995. Seismicity and P-wave velocity image of the Southern Tyrrhenian subduction zone. Geophys. J. Int. 121, 818–826.
Sibson, R.H., 2000. Fluid involvement in normal faulting. J. Geodyn. 29, 469–499.
Sibson, R.H., 2007. An episode of fault-valve behaviour during compressional inversion?—The 2004 M_j 6.8 Mid-Niigata Prefecture, Japan, earthquake sequence. Earth Planet. Sci. Lett. 257, 188–199.
Sigmundsson, F., Einarsson, P., Rögnvaldsson, S.Th., Foulger, G.R., Hodgkinson, K.M., Thorbergsson, G., 1997. The 1994–1995 seismicity and deformation at the Hengill triple junction, Iceland: triggering of earthquakes by minor magma injection in a zone of horizontal shear stress. J. Geophys. Res. 102, 15,151–15,161.
Sinclair, A.J., 1974. Selection of thresholds in geochemical data using probability graphs. J. Geochem. Explor. 3, 129–149.
Špičák, A., Horálek, J., 2001. Possible role of fluids in the process of earthquake swarm generation in the west Bohemia/Vogtland area. Tectonophysics 336, 151–161.
Tonani, F., Miele, G., 1991. Methods for Measuring Flow of Carbon Dioxide through Soils in the Volcanic Setting. Istituto di Analisi Globale e Applicazioni C.N.R., Firenze, Italy.
Tsujiura, M., 1983a. Waveform and spectral features of earthquake swarms and foreshocks: in special reference to earthquake prediction. Bull. Earthq Res. Inst. Tokyo Univ. 58, 65–133.
Tsujiura, M., 1983b. Characteristic frequencies for earthquake families and their tectonic implications: evidence from earthquake swarms in the Kanto District Japan. Pure Appl. Geophys. 4, 573–600.
Valensise, G., Pantosti, D., 1992. A 125 Kyr-long geological record of seismic source repeatability: the Messina Straits (southern Italy) and the 1908 earthquake (M_S=7.5). Terra Nova 4, 472–483.
Waldhauser, F., Ellsworth, W.L., 2000. A double-difference earthquake location algorithm: method and application to North Hayward Fault, California. Bull. Seismol. Soc. Am. 90, 1353–1368.
Zencher, F., Bonafede, M., Stefansson, R., 2006. Near-lithostatic pore pressure at seismogenic depths: a thermoporoelastic model. Geophys. J. Int. 166, 1318–1334.
Zito, G., Mongelli, F., De Lorenzo, S., Doglioni, C., 2003. Heat flow and geodynamics in the Tyrrhenian Sea. Terra Nova 15, 425–432. doi:10.1046/j.1365-3121.2003.00507.x.
Zoback, M., 2000. Strength of the San Andreas. Nature 44, 31–32.